



## RESEARCH PAPER

# CO<sub>2</sub> modulation of the rates of photosynthesis and light-dependent O<sub>2</sub> consumption in *Trichodesmium*

Tobias G. Boatman<sup>1,2,\*</sup>, Phillip A. Davey<sup>1</sup>, Tracy Lawson<sup>1</sup> and Richard J. Geider<sup>1</sup>

<sup>1</sup> School of Biological Sciences, University of Essex, Wivenhoe Park, Colchester CO4 3SQ, UK

<sup>2</sup> Department of Chemical Engineering, Imperial College London, South Kensington, London SW7 2AZ, UK

\* Correspondence: [t.boatman@imperial.ac.uk](mailto:t.boatman@imperial.ac.uk)

Received 6 June 2018; Editorial decision 15 October 2018; Accepted 23 October 2018

Editor: Howard Griffiths, University of Cambridge, UK.

## Abstract

As atmospheric CO<sub>2</sub> concentrations increase, so too does the dissolved CO<sub>2</sub> and HCO<sub>3</sub><sup>-</sup> concentrations in the world's oceans. There are still many uncertainties regarding the biological response of key groups of organisms to these changing conditions, which is crucial for predicting future species distributions, primary productivity rates, and biogeochemical cycling. In this study, we established the relationship between gross photosynthetic O<sub>2</sub> evolution and light-dependent O<sub>2</sub> consumption in *Trichodesmium erythraeum* IMS101 acclimated to three targeted pCO<sub>2</sub> concentrations (180 μmol mol<sup>-1</sup>=low-CO<sub>2</sub>, 380 μmol mol<sup>-1</sup>=mid-CO<sub>2</sub>, and 720 μmol mol<sup>-1</sup>=high-CO<sub>2</sub>). We found that biomass- (carbon) specific, light-saturated maximum net O<sub>2</sub> evolution rates (P<sub>nC,max</sub>) and acclimated growth rates increased from low- to mid-CO<sub>2</sub>, but did not differ significantly between mid- and high-CO<sub>2</sub>. Dark respiration rates were five times higher than required to maintain cellular metabolism, suggesting that respiration provides a substantial proportion of the ATP and reductant for N<sub>2</sub> fixation. Oxygen uptake increased linearly with gross O<sub>2</sub> evolution across light intensities ranging from darkness to 1100 μmol photons m<sup>-2</sup> s<sup>-1</sup>. The slope of this relationship decreased with increasing CO<sub>2</sub>, which we attribute to the increased energetic cost of operating the carbon-concentrating mechanism at lower CO<sub>2</sub> concentrations. Our results indicate that net photosynthesis and growth of *T. erythraeum* IMS101 would have been severely CO<sub>2</sub> limited at the last glacial maximum, but that the direct effect of future increases of CO<sub>2</sub> may only cause marginal increases in growth.

**Keywords:** Carbon fixation, CO<sub>2</sub>, cyanobacteria, gross photosynthesis, net photosynthesis, ocean acidification, *Trichodesmium*.

## Introduction

The ocean is one of the largest readily exchangeable reservoirs of inorganic carbon on Earth and is a major sink for anthropogenic CO<sub>2</sub> emissions (Sabine *et al.*, 2004). The ocean's capacity to sequester atmospheric CO<sub>2</sub> is strongly mediated by biological processes (Raven and Falkowski, 1999), where organic matter production and export drive CO<sub>2</sub> sequestration. This is important as future emission scenarios predict that atmospheric CO<sub>2</sub> will increase from present concentrations

(~400 μmol mol<sup>-1</sup>) to 750 μmol mol<sup>-1</sup> or 1000 μmol mol<sup>-1</sup> by the end of this century (Raven *et al.*, 2005). This will lead to an increase in the total dissolved inorganic carbon (TIC) in the surface ocean, reducing the pH from an average value of ~8.2 (pre-industrial) to ~7.9 (estimated for 2100) (Zeebe *et al.*, 1999; Zeebe and Wolf-Gladrow, 2001). Ocean acidification therefore favours an increase in seawater CO<sub>2</sub> and HCO<sub>3</sub><sup>-</sup> concentration and a decrease in pH and CO<sub>3</sub><sup>2-</sup>.

There are still many uncertainties regarding the biological response of key groups of organisms to these changing conditions, which is crucial for predicting future species distributions, primary productivity rates, and biogeochemical cycling. One group of great importance are diazotrophic cyanobacteria (photosynthetic dinitrogen fixers), as they contribute significantly to overall marine primary productivity by providing new nitrogen to many oligotrophic areas of the oceans. The filamentous cyanobacteria *Trichodesmium* are a colony-forming species that forms extensive surface blooms in the tropical and subtropical oceans (Carpenter and Capone, 1992; Capone *et al.*, 1997; Campbell *et al.*, 2005). *Trichodesmium* plays a significant role in the N cycle of the oligotrophic oceans; fixing nitrogen in an area corresponding to half of the Earth's surface (Davis and McGillicuddy, 2006) and representing up to 50% of new production in some oligotrophic tropical and subtropical oceans (Capone, 2005). The annual marine N<sub>2</sub> fixation is currently estimated at between 100 Tg and 200 Tg N per year (Gruber and Sarmiento, 1997; Karl *et al.*, 2002), of which *Trichodesmium* spp. contribute between 80 Tg and 110 Tg of fixed N<sub>2</sub> to open ocean ecosystems (Capone *et al.*, 1997).

Cyanobacteria have performed oxygenic photosynthesis for ~2.7 billion years (Buick, 2008). During that time, CO<sub>2</sub> concentrations have declined and O<sub>2</sub> concentrations increased, thus exerting an evolutionary pressure to form a mechanism to reduce the impact of photorespiration on photosynthetic CO<sub>2</sub> fixation. Despite cyanobacterial Rubisco having a relatively low affinity for CO<sub>2</sub>, cyanobacteria achieve high photosynthetic rates by virtue of an intracellular carbon-concentrating mechanism (CCM), which thereby reduces the diversion of energy into oxygenation of ribulose-1,5-bisphosphate (RuBP), the first step in photorespiration (Schwarz *et al.*, 1995; Kaplan and Reinhold, 1999). In addition, the CCM can aid in the dissipation of excess light energy as well as maintaining an optimal intracellular pH (Badger *et al.*, 1994; Kaplan and Reinhold, 1999).

Cyanobacteria have a unique ability to perform both photosynthesis and respiration simultaneously in the same cellular compartment (Nagarajan and Pakrasi, 2001). The thylakoid membranes of cyanobacteria contain both respiratory and photosynthetic electron transport chains, sharing the plastoquinone and plastocyanin pools and the Cyt *b<sub>6</sub>f* complex. In contrast, the cytoplasmic membrane is only capable of performing respiratory electron transport (Nagarajan and Pakrasi, 2001). Thus, it is common in cyanobacteria for respiratory electron transport to be inhibited at low light intensities as photosynthesis increases in the thylakoid membranes (Kana, 1992). However, in *Trichodesmium* there remains the possibility that photosynthetic and respiratory metabolism differs between diazocytes (where N<sub>2</sub> fixation occurs) and other cells within a trichome.

Previous studies report an increase in growth and productivity (CO<sub>2</sub> and N<sub>2</sub> fixation) of *T. erythraeum* IMS101 as well as changing elemental composition in response to future CO<sub>2</sub> concentrations (~750–1000 μmol mol<sup>-1</sup>) (Barcelos e Ramos *et al.*, 2007; Levitan *et al.*, 2007, 2010a; Kranz *et al.*, 2010; Spungin *et al.*, 2014; Hutchins *et al.*, 2015; Boatman *et al.*, 2017, 2018a, b), although, as discussed in Boatman *et al.* (2018a), the magnitude of the responses often differs between studies. Due to the significant contribution that *Trichodesmium* makes to

biogeochemical cycles and the predicted change in inorganic carbon (Ci) speciation over the coming decades, we performed a systematic experiment to assess how the photosynthetic physiology of *T. erythraeum* IMS101 was affected by acclimation to varying CO<sub>2</sub>. We ensured that the Ci chemistry and all other growth conditions were well defined, with cultures fully acclimated over long time periods (~5 months) to achieve balanced growth. We assessed the dark respiration, light absorption, and the light dependencies of gross O<sub>2</sub> evolution and O<sub>2</sub> consumption across different CO<sub>2</sub> conditions. We discuss how the responses that we observed may be related to N<sub>2</sub> fixation and changes in the cost of operating the CCM.

## Materials and methods

*Trichodesmium erythraeum* IMS101 was semi-continuously cultured to achieve fully acclimated balanced growth at three target pCO<sub>2</sub> concentrations (180, 380, and 720 μmol mol<sup>-1</sup>), under saturating light intensity (400 μmol photons m<sup>-2</sup> s<sup>-1</sup>), a 12/12 h light/dark (L/D) cycle, and an optimum growth temperature (26 ± 0.7 °C) for ~5 months (~40, 70, and 80 generations at low-, mid-, and high-CO<sub>2</sub>, respectively).

### Experimental set-up

Cultures of *T. erythraeum* IMS101 were grown in standard YBCII medium (Chen *et al.*, 1996) under diazotrophic conditions (N<sub>2</sub> only) in 1.5 litre volumes in 2 litre Pyrex bottles that had been acid-washed and autoclaved prior to culturing. Illumination was provided side-on by fluorescent tubes (Sylvania Luxline Plus FHQ49/T5/840). Cultures were constantly mixed using magnetic PTFE stirrer bars and aerated with a filtered (0.2 μm pore) air mixture at a rate of ~200 ml s<sup>-1</sup>. The CO<sub>2</sub> concentration was regulated (±2 μmol mol<sup>-1</sup>) by mass-flow controllers (Bronkhorst, Newmarket, UK) and CO<sub>2</sub>-free air was supplied by an oil-free compressor (Bambi Air, UK) via a soda-lime gas-tight column that was mixed with a 10% CO<sub>2</sub>-in-air mixture from a gas cylinder (BOC Industrial Gases, UK). The CO<sub>2</sub> concentration in the gas phase was continuously monitored by an infra-red gas analyser (Li-Cor Li-820, Lincoln, NE, USA), calibrated weekly against a standard gas (BOC Industrial Gases).

Cultures were kept at the upper section of the exponential growth phase through periodic dilution with new growth media at 3–5 d intervals. Daily growth rates were quantified from changes in baseline fluorescence (*F<sub>o</sub>*) measured between 09.00 h and 10.30 h on dark-adapted cultures (20 min) using a FRRfII FastAct Fluorometer System (Chelsea Technologies Group Ltd, UK). As detailed in Boatman *et al.* (2018a), cultures were deemed fully acclimated and in balanced growth when both the slope of the linear regression of ln(*F<sub>o</sub>*) and the ratio of live-cell to acetone-extracted *F<sub>o</sub>* were constant following every dilution with fresh YBCII medium.

The Ci chemistry was measured prior to the dilution of each culture with fresh media, where exactly 20 ml of culture from each treatment was filtered through a swinnex filter (25 mm, 0.45 μm pore, glass fibre filter): 15 ml into a plastic centrifuge tube (no headspace) for TIC analysis (Shimadzu TOC-V Analyser & ASI-V Autosampler), and 5 ml into a plastic cryogenic vial (Sigma-Aldrich V5257-250EA; no headspace) for pH analysis. The bicarbonate (HCO<sub>3</sub><sup>-</sup>), carbonate (CO<sub>3</sub><sup>2-</sup>), and CO<sub>2</sub> concentrations were calculated via CO<sub>2</sub>SYN as described in Boatman *et al.* (2017). Overall, the CO<sub>2</sub> drawdown in the cultures ranged between 49 μmol mol<sup>-1</sup> and 90 μmol mol<sup>-1</sup> for all CO<sub>2</sub> treatments (Table 1) and exhibited a negligible CO<sub>2</sub> drift over a diurnal cycle (see Supplementary Fig. S1 at JXB online).

### Gross and net O<sub>2</sub> exchange

Light-dependent rates of O<sub>2</sub> production and consumption were measured on four biological replicates per CO<sub>2</sub> treatment, using a membrane inlet mass spectrometer (MIMS) and an <sup>18</sup>O<sub>2</sub> technique modified from McKew *et al.* (2013).

**Table 1.** The growth conditions ( $\pm$ SE) achieved for *T. erythraeum* IMS101 when cultured at three target gas phase  $\text{CH}_2\text{CO}_2$  concentrations (low=180  $\mu\text{mol mol}^{-1}$ , mid=380  $\mu\text{mol mol}^{-1}$ , and high=720  $\mu\text{mol mol}^{-1}$ ), saturating light intensity (400  $\mu\text{mol photons m}^{-2} \text{s}^{-1}$ ), and optimal temperature (26 °C)

Variables	Units	Low-CO <sub>2</sub>	Mid-CO <sub>2</sub>	High-CO <sub>2</sub>
pH	–	8.461	8.175	7.905
H <sup>+</sup>	nM	3.5 (0.1)	6.7 (0.1)	12.5 (0.2)
A <sub>T</sub>	$\mu\text{M}$	2427 (32)	2490 (51)	2444 (42)
TCO <sub>2</sub>	$\mu\text{M}$	1797 (30)	2076 (44)	2204 (37)
HCO <sub>3</sub> <sup>–</sup>	$\mu\text{M}$	1356 (30)	1773 (37)	2008 (32)
CO <sub>3</sub> <sup>2–</sup>	$\mu\text{M}$	436 (9)	295 (8)	179 (5)
CO <sub>2</sub>	$\mu\text{M}$	3.3 (0.2)	8.2 (0.2)	17.4 (0.3)
NH <sub>4</sub> <sup>+</sup>	mM	1.00 (0.12)	1.06 (0.08)	1.02 (0.06)
NO <sub>3</sub> <sup>–</sup>	mM	0.33 (0.05)	0.36 (0.02)	0.32 (0.02)
<i>n</i>		76	32	28

Individual pH values were converted to a H<sup>+</sup> concentration, allowing a mean pH value to be calculated. Dissolved inorganic NH<sub>4</sub><sup>+</sup> was determined using the phenol-hypochlorite method as described by Solorzano (1969), while dissolved inorganic NO<sub>3</sub><sup>–</sup> was determined using the spectrophotometric method as described by Collos *et al.* (1999).

MIMS samples were prepared by placing 300 ml of culture in a large gas-tight syringe, and gently bubbled with N<sub>2</sub> gas for ~20 min to reduce the <sup>16</sup>O<sub>2</sub> concentration. The headspace was removed, and 2 ml of <sup>18</sup>O<sub>2</sub> gas (CK Gas Products, UK; 99% purity) was added and mixed by continuously inverting the syringe for 20 min. During this process, the culture was maintained at a low light intensity (<10  $\mu\text{mol photons m}^{-2} \text{s}^{-1}$ ) and at growth temperature (26 °C). Samples were incubated using a series of 6 ml glass stopper, gas-tight test tubes, which were cleaned with detergent, acid-washed (10% HCl for 1 d), and rinsed with deionized water (Millipore Milli-Q Biocel, ZMQS60FOI) prior to use. Glass beads were placed inside each test tube, allowing the sample to be mixed throughout the incubation. The <sup>18</sup>O<sub>2</sub>-enriched culture was quickly dispensed into the gas-tight glass test tubes, sealed using ground glass stoppers (no headspace), and immediately placed into a temperature-controlled (26 °C) incubator. A white light-emitting diode (LED) block (Iso Light 400, Technologica, Essex, UK) was positioned at one end of the incubator, generating light intensities ranging from 10  $\mu\text{mol photons m}^{-2} \text{s}^{-1}$  to 1100  $\mu\text{mol photons m}^{-2} \text{s}^{-1}$ .

For each replicate, 24 test tubes were incubated across the light gradient, a minimum of 10 test tubes were used to determine the initial concentration of O<sub>2</sub> isotopes, and an additional four test tubes were incubated in the dark (26 °C) to determine dark respiration rates. All photosynthesis–light (P–E) response curves were measured at the same time of day between 4 h and 6 h into the photo-phase of the L/D cycle and were incubated for between 60 min and 120 min. Culture densities for these experiments ranged from 80  $\mu\text{g Chl } a \text{ l}^{-1}$  to 240  $\mu\text{g Chl } a \text{ l}^{-1}$ .

Changes in <sup>16</sup>O<sub>2</sub> and <sup>18</sup>O<sub>2</sub> and thus O<sub>2</sub> consumption (U<sub>0</sub>) and O<sub>2</sub> evolution (E<sub>0</sub>) were calculated using the following equations (Radmer and Kok, 1976);

$$U_0 = - \left( 1 + \frac{^{16}\text{O}_2}{^{18}\text{O}_2} \right) \cdot \frac{\Delta ^{18}\text{O}_2}{\Delta t} \quad (1)$$

$$E_0 = \frac{\Delta ^{16}\text{O}_2}{\Delta t} - \left( \frac{^{16}\text{O}_2}{^{18}\text{O}_2} \right) \cdot \frac{\Delta ^{18}\text{O}_2}{\Delta t} \quad (2)$$

where U<sub>0</sub> is the rate of O<sub>2</sub> consumption and E<sub>0</sub> is the rate of gross O<sub>2</sub> evolution. C-specific rates were obtained by dividing U<sub>0</sub> and E<sub>0</sub> by the concentration of particulate organic carbon (POC). Rates were also normalized to Chl *a* and particulate organic nitrogen (PON), and are presented in Supplementary Figs S2 and S3.

The P–E curves for gross (E<sub>0C</sub>) and net O<sub>2</sub> exchange (P<sub>nC</sub>=E<sub>0C</sub>–U<sub>0C</sub>) were fitted to the following equations from Platt and Jassby (1976);

$$E_{0C} = E_{0C,\text{max}} \cdot \left[ 1 - e \left( \frac{-\alpha_{gC} \cdot E}{E_{0C,\text{max}}} \right) \right] \quad (3)$$

$$P_{nC} = P_{nC,\text{max}} \cdot \left[ 1 - e \left( \frac{-\alpha_{nC} \cdot E}{P_{nC,\text{max}}} \right) \right] + R_{dC} \quad (4)$$

where E<sub>0C,max</sub> and P<sub>nC,max</sub> are the carbon-specific maximum gross and net O<sub>2</sub> evolution rates;  $\alpha_{gC}$  and  $\alpha_{nC}$  are the carbon-specific initial light-limited slopes for gross and net photosynthesis; R<sub>dC</sub> is the dark respiration rate; and  $\bar{E}$  is the light intensity ( $\mu\text{mol photons m}^{-2} \text{s}^{-1}$ ). Curve fitting was performed on each biological replicate separately to calculate mean ( $\pm$ SE) curve fit parameterizations (Sigmaplot 11.0).

The maximum quantum efficiencies of gross ( $\phi_{m,g}$ ) and net ( $\phi_{m,n}$ ) O<sub>2</sub> evolution were calculated as follows;

$$\phi_{m,g} = \frac{\alpha_{gC}}{a_{C,\text{eff}}} \quad (5)$$

$$\phi_{m,n} = \frac{\alpha_{nC}}{a_{C,\text{eff}}} \quad (6)$$

where the C-specific initial slope for gross ( $\alpha_{gC}$ ) or net ( $\alpha_{nC}$ ) O<sub>2</sub> evolution, spectrally corrected to the culturing LEDs (Supplementary Fig. S6), was divided by the C-specific, spectrally corrected effective light absorption coefficient ( $a_{C,\text{eff}}$ ).

#### Spectrophotometric Chl *a* and POC analysis

Samples for the determination of Chl *a* and POC were collected with each light–response curve, while PON was calculated from the measured POC using the CO<sub>2</sub>-specific C:N ratio reported in Boatman *et al.* (2018a). For measurements of Chl *a* and POC, two 100 ml samples from each culture were vacuum-filtered onto pre-combusted 25 mm glass fibre filters (0.45  $\mu\text{m}$  pore; Fisherbrand FB59451, UK). The first filter was dried at 60 °C and the POC quantified using a TC analyser (Shimadzu TOC-V Analyser & SSM-5000A Solid Sample Combustion Unit). The second filter was placed in 5 ml of 100% methanol, homogenized, and extracted overnight at –20 °C, before being centrifuged at 12 000 g for 10 min, and a 3 ml aliquot of the supernatant added to a quartz cuvette. The absorption spectrum (400–800 nm) was measured using a (Hitachi U-3000, Japan) spectrophotometer and the Chl *a* concentration ( $\mu\text{g l}^{-1}$ ) was calculated using the following equation (Ritchie, 2008);

$$\text{Chl } a = \left[ \frac{(12.9447 \cdot (\text{Abs}_{665} - \text{Abs}_{750})) \cdot \text{Vol}_E}{\text{Vol}_F} \right] \cdot 1000 \quad (7)$$

where Abs<sub>665</sub> and Abs<sub>750</sub> are the baseline-corrected optical densities of the methanol-extracted sample at 665 nm and 750 nm; Vol<sub>E</sub> is the volume of the solvent used for extraction (i.e. 5 ml); Vol<sub>F</sub> is the volume of culture filtered (i.e. 100 ml), and 12.9447 is a cyanobacteria-specific Chl *a* coefficient for 100% methanol extraction.

Supporting spectrophotometric measurements were made on live cells using an integrating sphere to determine the *in vivo* light absorption (Supplementary File S1). From this we determined biomass-specific (Chl *a*, C, and N) light absorption coefficients under the varying CO<sub>2</sub> treatments (Supplementary Fig. S4), reconstructed the light absorption spectra from photosynthetic pigment spectra (Supplementary File SII; Supplementary Table S1), and calculated maximum quantum efficiencies of gross and net O<sub>2</sub> evolution (Table 3).

## Results

### Growth rate, cell composition, and light absorption

Balanced growth rates increased from 0.2 d<sup>-1</sup> at low-CO<sub>2</sub> to 0.34 d<sup>-1</sup> at mid-CO<sub>2</sub> and 0.36 d<sup>-1</sup> at high-CO<sub>2</sub> (Table 2). Chl *a*:C ratios were lowest under low-CO<sub>2</sub> conditions and were significantly higher in the mid-CO<sub>2</sub> treatment relative to the low- and high-CO<sub>2</sub> treatments (Table 2).

### Light dependence of O<sub>2</sub> exchange

The C-specific maximum rate (E<sub>0C,max</sub>) and initial slope (α<sub>gC</sub>) of light-dependent gross photosynthesis were significantly higher in the mid-CO<sub>2</sub> treatment relative to the low- and high-CO<sub>2</sub> treatments (Table 3). Conversely, the light saturation parameter (E<sub>k</sub>=E<sub>0C,max</sub>/α<sub>gC</sub>) for gross O<sub>2</sub> evolution (Table 3) and the maximum quantum efficiency of gross O<sub>2</sub> evolution (φ<sub>m,g</sub>=α<sub>gC</sub>/a<sub>C,eff</sub>) (Table 3) did not vary significantly amongst the CO<sub>2</sub> treatments due to co-variation of α<sub>gC</sub> and E<sub>0C,max</sub>.

**Table 2.** The mean (±SE) balanced growth rate and Chl *a*:C ratio for *T. erythraeum* IMS101 when acclimated to three target CO<sub>2</sub> concentrations (low=180 μmol mol<sup>-1</sup>, mid=380 μmol mol<sup>-1</sup>, and high=720 μmol mol<sup>-1</sup>), saturating light intensity (400 μmol photons m<sup>-2</sup> s<sup>-1</sup>), and optimal temperature (26 °C)

Variables	Units	Low-CO <sub>2</sub>	Mid-CO <sub>2</sub>	High-CO <sub>2</sub>
Growth rate	d <sup>-1</sup>	0.198 (0.027) A	0.336 (0.026) B	0.361 (0.020) B
Chl <i>a</i> :C	g:mol	0.052 (0.003) A	0.089 (0.003) C	0.066 (0.003) B

Abbreviations: Chl *a*:C ratios are g:mol (*n*=9 at low-CO<sub>2</sub>, *n*=6 at mid- and high-CO<sub>2</sub>). Letters indicate significant differences between CO<sub>2</sub> treatments (one-way ANOVA, Tukey post-hoc test; *P*<0.05); where B is significantly greater than A, and C is significantly greater than B and A.

**Table 3.** The physiological parameters (±SE) of the C-specific light-response curves for the gross and net photosynthetic O<sub>2</sub> evolution of *T. erythraeum* IMS101 (*n*=4) measured using the MIMS light source

Parameters	Units	Low-CO <sub>2</sub>	Mid-CO <sub>2</sub>	High-CO <sub>2</sub>
Gross O <sub>2</sub> evolution				
E <sub>0C,max</sub>	mmol O <sub>2</sub> (g C) <sup>-1</sup> h <sup>-1</sup>	1.875 (0.118) A	3.795 (0.175) C	2.973 (0.158) B
E <sub>k</sub>	μmol photons m <sup>-2</sup> s <sup>-1</sup>	277 (15)	250 (20)	281 (15)
α <sub>gC</sub>	μmol O <sub>2</sub> (g C) <sup>-1</sup> h <sup>-1</sup> (μmol photons m <sup>-2</sup> s <sup>-1</sup> ) <sup>-1</sup>	6.78 (0.33) A	15.35 (0.82) C	10.58 (0.18) B
φ <sub>m,g</sub>	mol O <sub>2</sub> (mol photons) <sup>-1</sup>	0.037 (0.004)	0.042 (0.004)	0.045 (0.003)
Net photosynthesis				
P <sub>nC,max</sub>	mmol O <sub>2</sub> (g C) <sup>-1</sup> h <sup>-1</sup>	1.131 (0.061) A	2.534 (0.287) B	2.312 (0.140) B
E <sub>k</sub>	μmol photons m <sup>-2</sup> s <sup>-1</sup>	300 (41)	270 (24)	270 (10)
α <sub>nC</sub>	μmol O <sub>2</sub> (g C) <sup>-1</sup> h <sup>-1</sup> (μmol photons m <sup>-2</sup> s <sup>-1</sup> ) <sup>-1</sup>	3.94 (0.46) A	9.48 (1.02) B	8.57 (0.35) B
R <sub>dC</sub>	mmol O <sub>2</sub> (g C) <sup>-1</sup> h <sup>-1</sup>	-0.600 (0.078)	-0.644 (0.132)	-0.659 (0.013)
φ <sub>m,n</sub>	mol O <sub>2</sub> (mol photons) <sup>-1</sup>	0.020 (0.002) A	0.026 (0.003) A	0.037 (0.002) B
Slopes				
P <sub>nC</sub> versus E <sub>0C</sub>	Dimensionless	0.571 (0.028) A	0.646 (0.046) A	0.791 (0.017) B
U <sub>0C</sub> versus E <sub>0C</sub>	Dimensionless	0.429 (0.028) B	0.354 (0.046) A	0.209 (0.017) A
U <sub>0C</sub> versus P <sub>nC</sub>	Dimensionless	0.701 (0.073) B	0.553 (0.111) B	0.254 (0.024) A

Abbreviations: E<sub>0C,max</sub>, the C-specific maximum gross O<sub>2</sub> evolution rate; P<sub>nC,max</sub>, the C-specific maximum net O<sub>2</sub> evolution rate; E<sub>k</sub>, the light saturation parameter; α<sub>gC</sub> and α<sub>nC</sub> are the C-specific initial slopes of the light-response curve for net and gross photosynthesis; φ<sub>m,g</sub> and φ<sub>m,n</sub> are the maximum quantum efficiencies of gross and net O<sub>2</sub> evolution calculated using the absorption coefficients reported in Supplementary Table S1; R<sub>dC</sub>, the C-specific dark respiration rate; Slope=the slope of the regression of E<sub>0C</sub> against P<sub>nC</sub>, E<sub>0C</sub> against O<sub>2</sub> uptake (U<sub>0C</sub>), and U<sub>0C</sub> against P<sub>nC</sub>. Letters indicate significant differences between CO<sub>2</sub> treatments (one-way ANOVA, Tukey post-hoc test; *P*<0.05); where B is significantly greater than A, and C is significantly greater than B and A.

The C:N ratios reported by Boatman et al. (2018a) for the low-, mid-, and high-CO<sub>2</sub> treatments (7.9, 7.8, and 7.3 mol:mol, respectively) were not significantly different. As such, the CO<sub>2</sub> response of N-specific maximum rates and light-limited initial slopes of gross O<sub>2</sub> evolution were comparable with C-specific rates (Supplementary Fig. S2; Supplementary Table S2). The ~2-fold variability of E<sub>0C,max</sub> and α<sub>gC</sub> was largely due to differences in the Chl *a*:C ratio, with the Chl *a*-specific light absorption varying by only 1% across CO<sub>2</sub> treatments (Supplementary Table S1).

The C-specific dark respiration rates (R<sub>dC</sub>) varied by ~10% amongst CO<sub>2</sub> treatments (Table 3). The maximum net O<sub>2</sub> evolution rate (P<sub>nC,max</sub>) approximately doubled from the low-CO<sub>2</sub> to the mid- and high-CO<sub>2</sub> treatments, but did not differ between mid- and high-CO<sub>2</sub>, with the initial slope (α<sub>nC</sub>) showing a similar pattern to P<sub>nC,max</sub> (Table 3). Similar responses were observed for the maximum rate (V<sub>C,max</sub>) and initial slope (Affinity) of the CO<sub>2</sub> dependency of C fixation as reported in Boatman et al. (2018a).

The relationship between P<sub>n</sub> and E<sub>0</sub> was linear (Fig. 1), with the slope increasing by ~13% from low- to mid-CO<sub>2</sub> and by 22% from mid- to high-CO<sub>2</sub> (Table 4). This linear relationship indicates that light-dependent O<sub>2</sub> consumption (U<sub>0C</sub>) was a constant proportion of gross O<sub>2</sub> evolution (E<sub>0C</sub>), independent of light intensity under each of the CO<sub>2</sub> treatments. Subtracting the slope from unity gives the ratio of light-dependent O<sub>2</sub> consumption to gross O<sub>2</sub> evolution, which declined significantly from 0.79 at high-CO<sub>2</sub> to 0.65 at mid-CO<sub>2</sub> and 0.57 at low-CO<sub>2</sub>.

### Photosynthetic quotient

We calculated the photosynthetic quotient (PQ) as:

$$PQ = \frac{P_{nC}}{V_C} \quad (8)$$



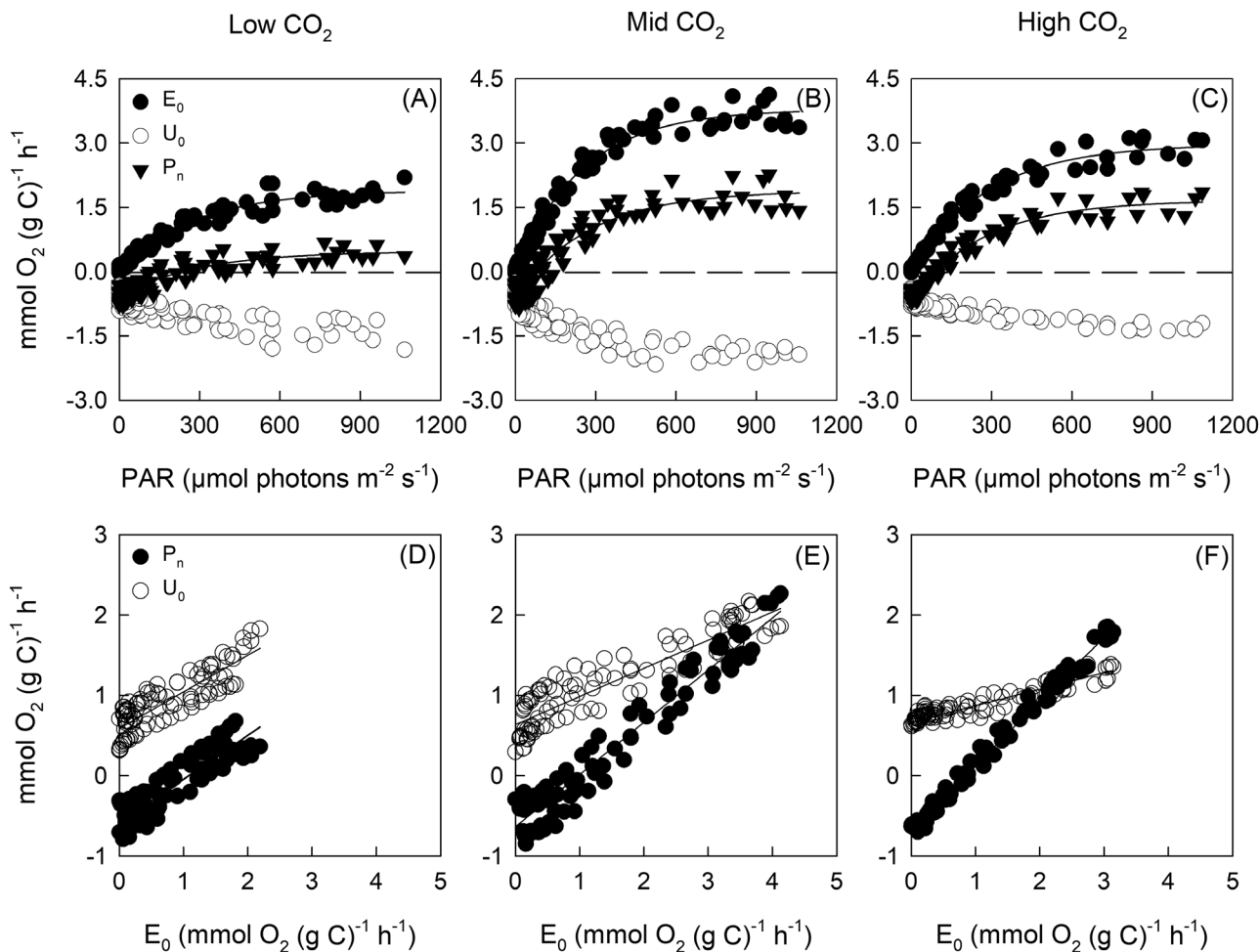


**Fig. 1.** The C-specific light–response curves for gross O<sub>2</sub> evolution, O<sub>2</sub> consumption, and net photosynthesis ( $n=4$ ) (A–C) and the relationship between gross net O<sub>2</sub> evolution and net O<sub>2</sub> evolution or O<sub>2</sub> consumption (D–F) for *T. erythraeum* IMS101. Oxygen evolution rates are normalized to a carbon basis [mmol O<sub>2</sub> (g C)<sup>-1</sup> h<sup>-1</sup>]. The dashed line represents where gross O<sub>2</sub> evolution equals O<sub>2</sub> consumption (i.e. net photosynthesis=0). Note, Chl *a*- and N-specific light–response curves are reported in [Supplementary Figs S2 and S3](#).

where  $P_{nC}$  is the C-specific net O<sub>2</sub> evolution rate ( $E_0 - U_0$ ) and  $V_C$  is the C-specific C-fixation rate reported by [Boatman \*et al.\* \(2018a\)](#), with both  $P_{nC}$  and  $V_C$  calculated at the growth light intensity (400 μmol photon m<sup>-2</sup> s<sup>-1</sup>) and growth CO<sub>2</sub> concentration (Table 1). The  $PQ$  calculated in this way (Table 4) did not vary systematically amongst the CO<sub>2</sub> treatments, averaging about 1.15 mol O<sub>2</sub> mol CO<sub>2</sub><sup>-1</sup>.

A second value of  $PQ$  was calculated by dividing  $E_{0C}$  by  $V_C$  for C fixation under the corresponding conditions, which increased from 1.3 mol O<sub>2</sub> mol CO<sub>2</sub><sup>-1</sup> in the high-CO<sub>2</sub> treatment to ~2.0 mol O<sub>2</sub> mol CO<sub>2</sub><sup>-1</sup> for the low- and mid-CO<sub>2</sub> treatments (Table 4), reflecting the increase in light-dependent O<sub>2</sub> consumption with decreasing CO<sub>2</sub>.

## Discussion

### *Effect of acclimation to variation of inorganic chemistry on growth rates and the Chl a:carbon ratio*

The increased growth rate from low- (180 μmol mol<sup>-1</sup>) to mid- (380 μmol mol<sup>-1</sup>) and high-CO<sub>2</sub> (720 μmol mol<sup>-1</sup>) was similar to previous findings ([Barcelos e Ramos \*et al.\*, 2007](#);

[Boatman \*et al.\*, 2017, 2018b](#)). Whilst not statistically significant, balanced growth rates were ~10% greater at high-CO<sub>2</sub> than at mid-CO<sub>2</sub>. The magnitude of this increase is comparable with several recent studies, which show rates increasing by 7–26% at similar CO<sub>2</sub> concentrations ([Barcelos e Ramos \*et al.\*, 2007](#); [Hutchins \*et al.\*, 2007](#); [Levitan \*et al.\*, 2007](#); [Kranz \*et al.\*, 2010](#); [Garcia \*et al.\*, 2011](#); [Boatman \*et al.\*, 2017](#)).

We observed that the Chl *a*:C ratio varied 1.7-fold, peaking in the mid-CO<sub>2</sub> treatment (Table 2). This is in contrast to previous research which showed that both Chl *a*:C and growth rate were largely independent of CO<sub>2</sub> in *Trichodesmium* ([Kranz \*et al.\*, 2009, 2010](#)). One possible explanation for the difference between our study and previous research is that we grew *Trichodesmium* at a higher light intensity (400 μmol photons m<sup>-2</sup> s<sup>-1</sup> in our experiments; 200 μmol photons m<sup>-2</sup> s<sup>-1</sup> used by [Kranz \*et al.\*](#)), and that pigment synthesis was down-regulated in our low-CO<sub>2</sub> treatment where CO<sub>2</sub> limited growth rate. Down-regulation of pigment synthesis by CO<sub>2</sub> limitation on growth was also observed previously for *Synechococcus* by [Fu \*et al.\* \(2007\)](#). In contrast, we hypothesize that the reduction in Chl *a*:C that we observed from mid-CO<sub>2</sub> to high-CO<sub>2</sub> may be due to the reduced cost of operating a CCM at high-CO<sub>2</sub>.

**Table 4.** The photosynthetic quotients ( $\pm$ SE) for *T. erythraeum* IMS101, calculated from the light-saturated, maximal rates of carbon-specific  $O_2$  evolution, and the C fixation rates

Parameters	Units	Low-CO <sub>2</sub>	Mid-CO <sub>2</sub>	High-CO <sub>2</sub>
Photosynthetic quotient				
$E_{0C}/V_C$	mol O <sub>2</sub> (mol C) <sup>-1</sup>	1.98 (0.10)	1.99 (0.04)	1.28 (0.04)
$P_{nC}/V_C$	mol O <sub>2</sub> (mol C) <sup>-1</sup>	1.14 (0.07)	1.29 (0.11)	1.01 (0.05)

$V_C$  was calculated as  $V_C = (V_{C,max} \times [CO_2]) / (K_m + [CO_2])$  using the value of  $K_m$  from Boatman et al. (2018a) and  $[CO_2]$  from Table 1.  $E_{0C}$  was calculated as  $E_{0C} = E_{0C,max} \times [1 - e^{-\alpha \times E / E_{0C,max}}]$  and  $P_{nC}$  was calculated as  $P_{nC} = P_{nC,max} \times [1 - e^{-\alpha \times E / P_{nC,max}}]$  using  $E = 400 \mu\text{mol photons m}^{-2} \text{ s}^{-1}$  and values of  $E_k$  from Table 3.

### Dark respiration and maintenance metabolic rate

Maintenance metabolism is a collection of key functions necessary to preserve cell viability that are commonly assumed to be independent of growth rate and as such can be estimated by extrapolating the relationship between light-limited growth rate and light intensity ( $E$ ) to  $E=0$  (Geider and Osborne, 1989). We estimated a maintenance metabolic rate [ $0.034 \text{ d}^{-1} \sim 0.12 \text{ mmol O}_2 (\text{g C})^{-1} \text{ h}^{-1}$ ] from previous observations of the light dependence of *Trichodesmium* growth (Boatman et al., 2017; Supplementary Fig. S5). In the dark, *Trichodesmium* has a respiration rate [ $R_d = 0.60\text{--}0.66 \text{ mmol O}_2 (\text{g cellular C})^{-1} \text{ h}^{-1}$ ] (Table 3) that is about five times higher than what is needed to maintain cellular metabolism. In most cyanobacteria, dark respiration rates ( $R_d$ ) are a small proportion of light-saturated net  $O_2$  production rates ( $P_{n,max}$ ) (Matthijs and Lubberding, 1988; Geider and Osborne, 1989). In contrast, we observed  $R_d$  rates that were a high proportion of light-saturated photosynthesis, consistent with other reports of high ratios of  $R_d$  to net photosynthesis in natural (Kana, 1993) and cultured *Trichodesmium* (Berman-Frank et al., 2001; Kranz et al., 2010; Eichner et al., 2017). For *Trichodesmium* spp., a high  $R_d$  is required to support the rates of  $N_2$  fixation measured in darkness.  $N_2$  fixation is energetically expensive, requiring a minimum consumption of 13 ATP and 6 reducing equivalents per  $N_2$  fixed, assuming complete recycling of  $H_2$  produced by nitrogenase to recover ATP.

From our observed growth rates and the C:N ratio reported by Boatman et al. (2018a), we calculate that the  $O_2$  consumption rate required to support the level of  $N_2$  fixation needed for growth is  $\sim 0.5 \text{ mmol O}_2 (\text{g C})^{-1} \text{ h}^{-1}$  in cells grown under low-CO<sub>2</sub>, increasing to  $\sim 1 \text{ mmol O}_2 (\text{g C})^{-1} \text{ h}^{-1}$  in cells grown under high-CO<sub>2</sub> (Supplementary File SIII). These rates are of the same order as  $R_d$  [ $0.60\text{--}0.66 \text{ mmol O}_2 (\text{g C})^{-1} \text{ h}^{-1}$ ] (Table 3), indicating that  $R_d$  may provide a substantial proportion of the ATP and reductant required for  $N_2$  fixation in the light. Significantly, Kana (1993) found that the addition of DCMU to illuminated cells caused the rate of oxygen uptake ( $U_0$ ) to decline to the rate observed in darkness, opening up the possibility that continuation of the 'dark' respiration rate in the light provides at least some of the energy required for  $N_2$  fixation.

### Effect of acclimation to $pCO_2$ on gross photosynthesis and photosynthetic quotients

Carbon-specific rates are directly related to changes in the specific growth rate, as both rates can be expressed in equivalent

units of inverse time (e.g.  $\text{h}^{-1}$  or  $\text{d}^{-1}$ ). However, due to differences in the Chl  $a$ :C ratio (Table 2), Chl  $a$ -specific maximum rates ( $E_{0Chl,max}$ ) and initial slopes ( $\alpha_{gChl}$ ) of light-dependent gross photosynthesis did not differ significantly between CO<sub>2</sub> treatments (Supplementary Fig. S3; Supplementary Table S3), an observation that is consistent with the findings reported by Levitan et al. (2007) and Eichner et al. (2014). We suggest that the reduced Chl  $a$ :C ratio at low-CO<sub>2</sub> relative to mid-CO<sub>2</sub> is probably due to the cost of up-regulating the CCM, whereas the reduced Chl  $a$ :C ratio at high-CO<sub>2</sub> relative to mid-CO<sub>2</sub> may be due to an increase in carbohydrate storage granules.

In contrast to  $E_{0C,max}$ , which clearly peaked in the mid-CO<sub>2</sub> treatment, the maximum net  $O_2$  evolution rate ( $P_{nC,max}$ ) increased from low- to mid-CO<sub>2</sub> but was not statistically different between mid- and high-CO<sub>2</sub> treatments (Table 3). The 2-fold increase of  $P_{nC,max}$  from low- to mid- and high-CO<sub>2</sub> is consistent with the effect of CO<sub>2</sub> on growth rate.

Dividing the rate of net  $O_2$  evolution ( $P_{nC}$ ) by the rate of C fixation under comparable light and CO<sub>2</sub> conditions gave values for the  $PQ$  that ranged from 1.0 mol  $O_2$  to 1.3 mol  $O_2$  evolved per mol  $CO_2$  fixed (Table 4). A  $PQ$  of 1.0 is expected if carbohydrate is the major product of photosynthesis as  $P_{nC}$  measures the light-driven electron transport from PSII to NADPH, which then feeds into  $CO_2$  assimilation by the Calvin cycle. A  $PQ > 1.0$  is expected if recent photosynthate is used in synthesis of compounds that are more reduced than carbohydrates (e.g. lipid) and/or that photosynthetically generated reductant is used to power  $N_2$  fixation and N assimilation into amino acids. Alternatively or in addition, a slightly higher  $PQ$  may be required if photosynthetically generated reductant is required for operation of the CCM, or for salvaging  $CO_2$  that leaks from carboxysomes by conversion of  $CO_2$  to  $HCO_3^-$  by NDH-I<sub>4</sub> (Price et al. (2008)). This corroborates our findings, where under high-CO<sub>2</sub>, when the CCM is probably down-regulated, we observed a  $PQ$  value close to 1.0. Conversely at low- and mid-CO<sub>2</sub>, when more energy is required for the CCM, we observed a  $PQ$  value  $> 1.0$ .

### Effect of acclimation to $pCO_2$ on light-stimulated $O_2$ consumption and the relationship between net and gross $O_2$ evolution

We found that  $O_2$  consumption rates ( $U_0$ ) of *Trichodesmium* increased markedly with light intensity, with  $U_0$  saturating at a similar light intensity to gross  $O_2$  evolution (Fig. 1). This suggests that light-driven  $U_0$  increased in parallel with gross  $O_2$  evolution and that dark respiration continued at similar rates in the light and dark. Previously, Kana (1993) observed a very slight decline in  $U_0$  between darkness and low-light intensity in natural *Trichodesmium* colonies, followed by parallel increases of  $U_0$  and  $O_2$  evolution ( $E_0$ ) with increasing light. Kana (1993) attributed the light-stimulated component of  $U_0$  to the Mehler reaction, as the addition of DCMU to illuminated cells caused  $U_0$  to decline to the rate observed in darkness.

The slope of the dependence of  $U_{0C}$  on  $E_{0C}$  decreased with increasing growth CO<sub>2</sub> from 0.43 in cultures grown under low-CO<sub>2</sub> to 0.21 in cultures grown under high-CO<sub>2</sub> (Table 3). Thus, the light-driven component of  $U_0$  decreased from  $\sim 43\%$  of  $E_0$  in the low-CO<sub>2</sub> culture to 21% of  $E_0$  in the high-CO<sub>2</sub>

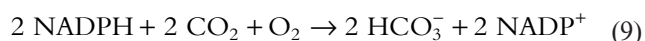
culture. Pseudocyclic photophosphorylation coupled to the consumption of O<sub>2</sub> associated with the Mehler reaction can provide ATP that may be used to support N<sub>2</sub> fixation, CO<sub>2</sub> fixation, or for operating a CCM (Miller *et al.*, 1988). The linearity between U<sub>0</sub> and E<sub>0</sub> suggests that light-dependent O<sub>2</sub> consumption may be required to balance the ratio of ATP production to NADPH production in the light reactions of photosynthesis. As the photon efficiency of ATP production by pseudocyclic photophosphorylation is the same as that of photophosphorylation driven by linear photosynthetic electron transport (LPET) (Baker *et al.*, 2007), our results suggest that 26% more ATP than can be generated by LPET is required by cells growing under high-CO<sub>2</sub>, increasing to 55% more ATP in cells growing under mid-CO<sub>2</sub> and 75% more ATP in cells growing under low-CO<sub>2</sub>. Much of the additional ATP that could be generated by pseudocyclic photophosphorylation may be accounted for by the ATP requirements for CO<sub>2</sub> fixation by the Calvin cycle (1.5 ATP/e<sup>-</sup>) and N<sub>2</sub> fixation (2.1 ATP/e<sup>-</sup>) being greater than the ratio of ATP to reducing equivalents generated by LPET (1.25 ATP/e<sup>-</sup>). At low-CO<sub>2</sub>, the increase in U<sub>0</sub> may also be required to operate a CCM, as observed in the freshwater *Synechococcus* (Miller *et al.*, 1988).

#### An estimate of the cost of operating the CCM

Stimulation of growth and productivity of *T. erythraeum* IMS101 in response to increasing CO<sub>2</sub> is commonly attributed to reductions in the amount of energy required for establishing, maintaining, and operating a CCM (Hutchins *et al.*, 2007, 2015; Levitan *et al.*, 2007; Garcia *et al.*, 2011). Two aspects for the cost of operating the CCM in *Trichodesmium* are those for HCO<sub>3</sub><sup>-</sup> transport into the cell, which must balance CO<sub>2</sub> fixation and CO<sub>2</sub> leakage, and those for retaining inorganic C within the cell by converting CO<sub>2</sub> that diffuses from the carboxysome to HCO<sub>3</sub><sup>-</sup> via the NDH-I<sub>4</sub> CO<sub>2</sub> uptake/salvage system. The cost of HCO<sub>3</sub><sup>-</sup> transport of ~1 ATP for each C transported into the cell (Raven *et al.*, 2014) could be supplied by either cyclic photosynthetic electron transfer around PSI or pseudocyclic photosynthetic electron transfer linked to the Mehler reaction. As the ratio of CO<sub>2</sub> leakage to gross inorganic C uptake has been found to be independent of pCO<sub>2</sub> over the range of 150–1000 μmol mol<sup>-1</sup> (Kranz *et al.*, 2009, 2010), the ATP required for HCO<sub>3</sub><sup>-</sup> transport will also be independent of pCO<sub>2</sub>.

Rather than fuelling ATP production by pseudocyclic electron transport, light-dependent O<sub>2</sub> consumption may be a consequence of operating the NDH-I<sub>4</sub> CO<sub>2</sub> uptake/salvage system. For *Trichodesmium*, the NDH-I<sub>4</sub> protein is thought to reduce the efflux of CO<sub>2</sub> from the cell, converting it to HCO<sub>3</sub><sup>-</sup> but at a cost of consuming reducing equivalents [NADPH or reduced ferredoxin (F<sub>d</sub>)] (Price *et al.*, 2008).

The stoichiometry based on NADPH as the electron donor can be represented as:



If NDH-I<sub>4</sub> activity is employed to minimize CO<sub>2</sub> effluxes, then the rate of O<sub>2</sub> consumption associated with this process would

be expected to decrease with increases of extracellular CO<sub>2</sub> concentration. As NADPH consumption by this mechanism is closely linked in time and space to NADPH production via LPET, this process would be inhibited by DCMU in a similar manner to the Mehler reaction.

#### Roles of photosynthetic and respiratory metabolism in N<sub>2</sub> fixation

Increased pCO<sub>2</sub> will not only stimulate CO<sub>2</sub> fixation, but will also stimulate N<sub>2</sub> fixation (dependent on carbon skeletons for sequestration of the ammonium produced) and growth in *Trichodesmium* (Barcelos e Ramos *et al.*, 2007; Hutchins *et al.*, 2007; Levitan *et al.*, 2007, 2010b; Kranz *et al.*, 2009, 2010). This is probably in response to energy relocation from the CCM (Badger *et al.*, 2006; Kranz *et al.*, 2011) toward CO<sub>2</sub> and N<sub>2</sub> fixation (Levitan *et al.*, 2007; Kranz *et al.*, 2011).

Diazocytes may use the light reactions of photosynthesis to provide some or most of the ATP required to support N<sub>2</sub> fixation either through cyclic photophosphorylation associated with electron transfer around PSI or through pseudocyclic photophosphorylation involving LPET from H<sub>2</sub>O to O<sub>2</sub> involving both PSII and PSI. However, LPET evolves O<sub>2</sub>, which is known to inactivate nitrogenase. Enhanced rates of the Mehler reaction, unless uncoupled from O<sub>2</sub> evolution at PSII, will not affect the O<sub>2</sub> balance of diazocytes. However, if respiration provides the ATP for N<sub>2</sub> fixation, then sugars and/or organic acids may be produced by photosynthesis in diazocytes prior to the initiation of N<sub>2</sub> fixation (temporal separation of CO<sub>2</sub> fixation from N<sub>2</sub> fixation) or in other cells within the trichome and transported laterally into the diazocytes (spatial separation of CO<sub>2</sub> fixation from N<sub>2</sub> fixation).

Temporal separation of N<sub>2</sub> fixation from photosynthetic O<sub>2</sub> evolution may be achieved if glycogen that accumulates in diazocytes prior to the onset of N<sub>2</sub> fixation provides the reducing equivalents and ATP to fuel N<sub>2</sub> fixation, perhaps supplemented by high rates of cyclic photosynthetic electron transfer around PSI to generate ATP. Temporal separation is consistent with the pattern of CO<sub>2</sub> fixation and N<sub>2</sub> fixation observed in *Trichodesmium* where the former peaks earlier in the day than the latter (Berman-Frank *et al.*, 2001). Spatial separation has been observed in heterocystous cyanobacteria where transport of sugars into heterocysts from surrounding cells can be respired to fuel N<sub>2</sub> fixation (Wolk, 1968; Böhme, 1998). Although we are not aware of direct evidence for rapid transfer of metabolites amongst cells along a trichome, such a transfer would be consistent with observations of Finzi-Hart *et al.* (2009), showing that all cells within a *Trichodesmium* trichome show the same temporal pattern of accumulation and mobilization of cyanophycin granules and the same temporal pattern of labelling with <sup>13</sup>CO<sub>2</sub> and <sup>15</sup>N.

#### Conclusion

In this study, we accredit the bell-shaped CO<sub>2</sub> response of the C-specific maximum gross photosynthesis rates (E<sub>0C,max</sub>) to the CCM, where the 2-fold increase in E<sub>0C,max</sub> from low- to mid-CO<sub>2</sub> supports the almost 2-fold increase in balanced growth rates



and the decrease in  $E_{0C,max}$  from mid- to high- $CO_2$  is due to less expenditure on the CCM whilst cells grow at a similar rate.

Our results indicate a significant decrease in the ratio of the rate of light-driven  $O_2$  consumption to the rate of gross photosynthetic  $O_2$  evolution with increasing  $CO_2$ , which probably arises from a reduced cost of operating the CCM. In addition, dark respiration appears to be sufficient to provide much of the energy required to support significant rates of  $N_2$  fixation, even in the light.

We have not extrapolated our findings to a full day as light–response curves were measured at one time point and *Trichodesmium* exhibits pronounced diurnal variability in photosynthesis and  $N_2$  fixation (Berman-Frank *et al.*, 2001). In addition, extrapolating to future conditions in the natural environment should consider (i) the impact of adaptation of *Trichodesmium* to future conditions (Hutchins *et al.*, 2015); (ii) strain and clade variability (Hutchins *et al.*, 2013); and (iii) additional integrated effects of abiotic variables other than  $CO_2$  (i.e. light intensity, temperature, and nutrients such as P and Fe) (Walworth *et al.*, 2016).

In the context of open oceans, nutrient-replete  $P_n$  and growth rates of *T. erythraeum* IMS101 would have been severely  $CO_2$  limited at the last glacial maximum relative to current conditions. Future increases of  $CO_2$  may not significantly increase growth and productivity of *Trichodesmium*, although increases in key stoichiometric ratios (N:P and C:P) as reported by Boatman *et al.* (2018a) may affect bacterial and zooplankton metabolism, the pool of bioavailable N, the depth at which sinking organic matter is remineralized, and consequently carbon sequestration via the biological carbon pump (Mulholland *et al.*, 2004; McGillicuddy, 2014). These responses could serve as a negative feedback to climate change by increasing new N and C production, thereby increasing the organic carbon sinking to the deep ocean.

## Supplementary data

Supplementary data are available at *JXB* online.

Table S1. The measured and modelled effective light absorption coefficients and relative photosynthetic pigment contribution to the total light absorption.

Table S2. The physiological parameters of the N-specific light–response curves for gross and net photosynthetic  $O_2$  evolution of *T. erythraeum* IMS101.

Table S3. The physiological parameters of the Chl *a*-specific light–response curves for gross and net photosynthetic  $O_2$  evolution of *T. erythraeum* IMS101.

Table S4. Values of the goodness of fit for the C-specific light–response curves for gross and net photosynthetic  $O_2$  evolution of *T. erythraeum* IMS101.

Table S5. The Chl *a*-specific photosynthetic quotients of *T. erythraeum* IMS101.

Fig. S1. The inorganic carbon chemistry of *T. erythraeum* IMS101 cultures over the light period.

Fig. S2. The N-specific light–response curves for gross  $O_2$  evolution,  $O_2$  consumption, and net photosynthesis for *T. erythraeum* IMS101.

Fig. S3. The Chl *a*-specific light–response curves for gross  $O_2$  evolution,  $O_2$  consumption, and net photosynthesis for *T. erythraeum* IMS101.

Fig. S4. The measured and modelled *in vivo* light absorption spectra for *T. erythraeum* IMS101.

Fig. S5. The light compensation point of *T. erythraeum* IMS101 growth.

Fig. S6. The relative emission spectra of the culturing and MIMS LEDs and the spectral corrected light absorption spectra of *T. erythraeum* IMS101.

File S1. *In vivo* light absorption.

File S2. Modelling the *in vivo* light absorption from pigment absorption spectra.

File S3. Stoichiometry and energetics of  $N_2$  fixation.

## Acknowledgements

TGB was supported by a UK Natural Environment Research Council PhD studentship (NE/J500379/1 DTB).

## References

- Badger MR, Palmqvist K, Yu JW. 1994. Measurement of  $CO_2$  and  $HCO_3^-$  fluxes in cyanobacteria and microalgae during steady-state photosynthesis. *Physiologia Plantarum* **90**, 529–536.
- Badger MR, Price GD, Long BM, Woodger FJ. 2006. The environmental plasticity and ecological genomics of the cyanobacterial  $CO_2$  concentrating mechanism. *Journal of Experimental Botany* **57**, 249–265.
- Baker NR, Harbinson J, Kramer DM. 2007. Determining the limitations and regulation of photosynthetic energy transduction in leaves. *Plant, Cell & Environment* **30**, 1107–1125.
- Barcelos e Ramos J, Biswas H, Schulz KG, LaRoche J, Riebesell U. 2007. Effect of rising atmospheric carbon dioxide on the marine nitrogen fixer *Trichodesmium*. *Global Biogeochemical Cycles* **21**, GB2028.
- Berman-Frank I, Lundgren P, Chen YB, Küpper H, Kolber Z, Bergman B, Falkowski P. 2001. Segregation of nitrogen fixation and oxygenic photosynthesis in the marine cyanobacterium *Trichodesmium*. *Science* **294**, 1534–1537.
- Boatman TG, Lawson T, Geider RJ. 2017. A key marine diazotroph in a changing ocean: the interacting effects of temperature,  $CO_2$  and light on the growth of *Trichodesmium erythraeum* IMS101. *PLoS One* **12**, e0168796.
- Boatman TG, Mangan NM, Lawson T, Geider RJ. 2018a. Inorganic carbon and pH dependency of photosynthetic rates in *Trichodesmium*. *Journal of Experimental Botany* **69**, 3651–3660.
- Boatman TG, Oxborough K, Gledhill M, Lawson T, Geider RJ. 2018b. An integrated response of *Trichodesmium erythraeum* IMS101 growth and photo-physiology to iron,  $CO_2$ , and light intensity. *Frontiers in Microbiology* **9**, 624.
- Böhme H. 1998. Regulation of nitrogen fixation in heterocyst-forming cyanobacteria. *Trends in Plant Science* **3**, 346–351.
- Buick R. 2008. When did oxygenic photosynthesis evolve? *Philosophical Transactions of the Royal Society B: Biological Sciences* **363**, 2731–2743.
- Campbell L, Carpenter E, Montoya J, Kustka A, Capone D. 2005. Picoplankton community structure within and outside a *Trichodesmium* bloom in the southwestern Pacific Ocean. *Vie et Milieu* **55**, 185–195.
- Capone DG. 2005. Nitrogen fixation by *Trichodesmium* spp.: an important source of new nitrogen to the tropical and subtropical North Atlantic Ocean. *Global Biogeochemical Cycles* **19**, GB2024.
- Capone DG, Zehr JP, Paerl HW, Bergman B, Carpenter EJ. 1997. *Trichodesmium*, a globally significant marine cyanobacterium. *Science* **276**, 1221–1229.
- Carpenter EJ, Capone DG. 1992. Nitrogen fixation in *Trichodesmium* blooms. In: Carpenter EJ, Capone DG, eds. *Marine pelagic cyanobacteria: Trichodesmium and other diazotrophs*. Dordrecht: Kluwer Academic Publishers, 211–217.



- Chen YB, Zehr JP, Mellon M.** 1996. Growth and nitrogen fixation of the diazotrophic filamentous nonheterocystous cyanobacterium *Trichodesmium* Sp. IMS 101 in defined media: evidence for a circadian rhythm. *Journal of Phycology* **32**, 916–923.
- Collos Y, Mornet F, Sciandra A, Waser N, Larson A, Harrison P.** 1999. An optical method for the rapid measurement of micromolar concentrations of nitrate in marine phytoplankton cultures. *Journal of Applied Phycology* **11**, 179–184.
- Davis CS, McGillicuddy DJ Jr.** 2006. Transatlantic abundance of the N<sub>2</sub>-fixing colonial cyanobacterium *Trichodesmium*. *Science* **312**, 1517–1520.
- Eichner MJ, Klawonn I, Wilson ST, Littmann S, Whitehouse MJ, Church MJ, Kuypers MM, Karl DM, Ploug H.** 2017. Chemical microenvironments and single-cell carbon and nitrogen uptake in field-collected colonies of *Trichodesmium* under different pCO<sub>2</sub>. *ISME Journal* **11**, 1305–1317.
- Eichner M, Kranz SA, Rost B.** 2014. Combined effects of different CO<sub>2</sub> levels and N sources on the diazotrophic cyanobacterium *Trichodesmium*. *Physiologia Plantarum* **152**, 316–330.
- Finzi-Hart JA, Pett-Ridge J, Weber PK, Popa R, Fallon SJ, Gunderson T, Hutcheon ID, Neelson KH, Capone DG.** 2009. Fixation and fate of C and N in the cyanobacterium *Trichodesmium* using nanometer-scale secondary ion mass spectrometry. *Proceedings of the National Academy of Sciences, USA* **106**, 6345–6350.
- Fu FX, Warner ME, Zhang Y, Feng Y, Hutchins DA.** 2007. Effects of increased temperature and CO<sub>2</sub> on photosynthesis, growth and elemental ratios of marine *Synechococcus* and *Prochlorococcus* (Cyanobacteria). *Journal of Phycology* **43**, 485–496.
- Garcia NS, Fu FX, Breene CL, Bernhardt PW, Mulholland MR, Sohm JA, Hutchins DA.** 2011. Interactive effects of irradiance and CO<sub>2</sub> on CO<sub>2</sub> fixation and N<sub>2</sub> fixation in the diazotroph *Trichodesmium erythraeum* (Cyanobacteria). *Journal of Phycology* **47**, 1292–1303.
- Geider RJ, Osborne BA.** 1989. Respiration and microalgal growth: a review of the quantitative relationship between dark respiration and growth. *New Phytologist* **112**, 327–341.
- Gruber N, Sarmiento JL.** 1997. Global patterns of marine nitrogen fixation and denitrification. *Global Biogeochemical Cycles* **11**, 235–266.
- Hutchins DA, Fu F-X, Webb EA, Walworth N, Tagliabue A.** 2013. Taxon-specific response of marine nitrogen fixers to elevated carbon dioxide concentrations. *Nature Geoscience* **6**, 790–795.
- Hutchins D, Fu FX, Zhang Y, Warner M, Feng Y, Portune K, Bernhardt P, Mulholland M.** 2007. CO<sub>2</sub> control of *Trichodesmium* N<sub>2</sub> fixation, photosynthesis, growth rates, and elemental ratios: implications for past, present, and future ocean biogeochemistry. *Limnology and Oceanography* **52**, 1293–1304.
- Hutchins DA, Walworth NG, Webb EA, Saito MA, Moran D, McIlvin MR, Gale J, Fu FX.** 2015. Irreversibly increased nitrogen fixation in *Trichodesmium* experimentally adapted to elevated carbon dioxide. *Nature Communications* **6**, 8155.
- Kana TM.** 1992. Relationship between photosynthetic oxygen cycling and carbon assimilation in *Synechococcus* WH7803 (Cyanophyta). *Journal of Phycology* **28**, 304–308.
- Kana TM.** 1993. Rapid oxygen cycling in *Trichodesmium thiebautii*. *Limnology and Oceanography* **38**, 18–24.
- Kaplan A, Reinhold L.** 1999. CO<sub>2</sub> concentrating mechanisms in photosynthetic microorganisms. *Annual Review of Plant Physiology and Plant Molecular Biology* **50**, 539–570.
- Karl D, Michaels A, Bergman B, Capone D, Carpenter E, Letelier R, Lipschultz F, Paerl H, Sigman D, Stal L.** 2002. Dinitrogen fixation in the world's oceans. *Biogeochemistry* **57**, 47–98.
- Kranz SA, Eichner M, Rost B.** 2011. Interactions between CCM and N<sub>2</sub> fixation in *Trichodesmium*. *Photosynthesis Research* **109**, 73–84.
- Kranz SA, Levitan O, Richter KU, Prášil O, Berman-Frank I, Rost B.** 2010. Combined effects of CO<sub>2</sub> and light on the N<sub>2</sub>-fixing cyanobacterium *Trichodesmium* MS101: physiological responses. *Plant Physiology* **154**, 334–345.
- Kranz SA, Sültemeyer D, Richter KU, Rost B.** 2009. Carbon acquisition in *Trichodesmium*: the effect of pCO<sub>2</sub> and diurnal changes. *Limnology and Oceanography* **54**, 548–559.
- Levitan O, Brown CM, Sudhaus S, Campbell D, LaRoche J, Berman-Frank I.** 2010a. Regulation of nitrogen metabolism in the marine diazotroph *Trichodesmium* IMS101 under varying temperatures and atmospheric CO<sub>2</sub> concentrations. *Environmental Microbiology* **12**, 1899–1912.
- Levitan O, Rosenberg G, Setlik I, Setlikova E, Grigel J, Klepetar J, Prasil O, Berman-Frank I.** 2007. Elevated CO<sub>2</sub> enhances nitrogen fixation and growth in the marine cyanobacterium *Trichodesmium*. *Global Change Biology* **13**, 531–538.
- Levitan O, Sudhaus S, LaRoche J, Berman-Frank I.** 2010b. The influence of pCO<sub>2</sub> and temperature on gene expression of carbon and nitrogen pathways in *Trichodesmium* IMS101. *PLoS One* **5**, e15104.
- Matthijs H, Lubberding H.** 1988. Dark respiration in cyanobacteria. In: **Rogers LJ, Gallon JR**, eds. *Biochemistry of the algae and cyanobacteria*. Proceedings of the Phytochemical Society of Europe. Oxford/New York: Clarendon Press, 131–145.
- McGillicuddy DJ.** 2014. Do *Trichodesmium* spp. populations in the North Atlantic export most of the nitrogen they fix? *Global Biogeochemical Cycles* **28**, 103–114.
- McKew BA, Davey P, Finch SJ, Hopkins J, Lefebvre SC, Metodiev MV, Oxborough K, Raines CA, Lawson T, Geider RJ.** 2013. The trade-off between the light-harvesting and photoprotective functions of fucoxanthin-chlorophyll proteins dominates light acclimation in *Emiliania huxleyi* (clone CCMP 1516). *New Phytologist* **200**, 74–85.
- Miller AG, Espie GS, Canvin DT.** 1988. Active transport of inorganic carbon increases the rate of O<sub>2</sub> photoreduction by the cyanobacterium *Synechococcus* UTEX 625. *Plant Physiology* **88**, 6–9.
- Mulholland MR, Bronk DA, Capone DG.** 2004. Dinitrogen fixation and release of ammonium and dissolved organic nitrogen by *Trichodesmium* IMS101. *Aquatic Microbial Ecology* **37**, 85–94.
- Nagarajan A, Pakrasi HB.** 2001. Membrane-bound protein complexes for photosynthesis and respiration in Cyanobacteria. *eLS* 1–8.
- Platt T, Jassby AD.** 1976. The relationship between photosynthesis and light for natural assemblages of coastal marine phytoplankton. *Journal of Phycology* **12**, 421–430.
- Price GD, Badger MR, Woodger FJ, Long BM.** 2008. Advances in understanding the cyanobacterial CO<sub>2</sub>-concentrating-mechanism (CCM): functional components, Ci transporters, diversity, genetic regulation and prospects for engineering into plants. *Journal of Experimental Botany* **59**, 1441–1461.
- Radmer RJ, Kok B.** 1976. Photoreduction of O<sub>2</sub> primes and replaces CO<sub>2</sub> assimilation. *Plant Physiology* **58**, 336–340.
- Raven JA, Beardall J, Giordano M.** 2014. Energy costs of carbon dioxide concentrating mechanisms in aquatic organisms. *Photosynthesis Research* **121**, 111–124.
- Raven J, Caldeira K, Elderfield H, Hoegh-Guldberg O, Liss P, Riebesell U, Shepherd J, Turley C, Watson A.** 2005. *Ocean acidification due to increasing atmospheric carbon dioxide*. London: The Royal Society.
- Raven J, Falkowski P.** 1999. Oceanic sinks for atmospheric CO<sub>2</sub>. *Plant, Cell & Environment* **22**, 741–755.
- Ritchie R.** 2008. Universal chlorophyll equations for estimating chlorophylls a, b, c, and d and total chlorophylls in natural assemblages of photosynthetic organisms using acetone, methanol, or ethanol solvents. *Photosynthetica* **46**, 115–126.
- Sabine CL, Feely RA, Gruber N, et al.** 2004. The oceanic sink for anthropogenic CO<sub>2</sub>. *Science* **305**, 367–371.
- Schwarz R, Reinhold L, Kaplan A.** 1995. Low activation state of ribulose-1,5-bisphosphate carboxylase/oxygenase in carboxysome-defective *Synechococcus* mutants. *Plant Physiology* **108**, 183–190.
- Solorzano L.** 1969. Determination of ammonia in natural waters by the phenol hypochlorite method. *Limnology and Oceanography* **14**, 799–801.
- Spungin D, Berman-Frank I, Levitan O.** 2014. *Trichodesmium*'s strategies to alleviate phosphorus limitation in the future acidified oceans. *Environmental Microbiology* **16**, 1935–1947.
- Walworth NG, Fu FX, Webb EA, Saito MA, Moran D, McIlvin MR, Lee MD, Hutchins DA.** 2016. Mechanisms of increased *Trichodesmium* fitness under iron and phosphorus co-limitation in the present and future ocean. *Nature communications* **7**, 12081.
- Wolk CP.** 1968. Movement of carbon from vegetative cells to heterocysts in *Anabaena cylindrica*. *Journal of Bacteriology* **96**, 2138–2143.
- Zeebe RE, Wolf-Gladrow DA.** 2001. *CO<sub>2</sub> in seawater: equilibrium, kinetics, isotopes*. Amsterdam: Elsevier Science.
- Zeebe RE, Wolf-Gladrow D, Jansen H.** 1999. On the time required to establish chemical and isotopic equilibrium in the carbon dioxide system in seawater. *Marine Chemistry* **65**, 135–153.